A novel scheme to measure 2D error motions of linear axes by regulating the direction of a laser interferometer

Soichi Ibaraki[a], Mashu Hiruya[b]

[a]*Department of Mechanical Systems Engineering, Hiroshima University*
Kagamiyama 1-4-1, Higashi Hiroshima, 739-8527, Japan. Phone/Fax: +81-82-424-7580
[b]*Department of Micro Engineering, Kyoto University*
Katsura, Nishigyo-ku, Kyoto 616-8540, Japan

Type of contribution: Original research paper

Abstract

In the standardized accuracy test procedures for machine tools, error motions of a linear axis, i.e. the linear positioning, straightness, and angular error motions, are separately measured in a different setup with a different measuring instrument. This paper presents a novel scheme to measure all the two-dimensional (2D) error motions of two linear axes by using a laser interferometer only. The proposed test consists of 1) direct measurement of the linear positioning deviation of two linear axes, and 2) the distance measurement to the retroreflector, positioned by the two linear axes on a rectangular path, by continuously regulating the laser beam direction of a laser interferometer. It requires a laser interferometer only; lower implementation cost is its major practical advantage. As an experimental case study, the proposed scheme is applied to a large-sized machine tool. The uncertainty analysis is also presented.

Keywords: machine tool, measurement, laser interferometer, volumetric accuracy, tracking interferometer, kinematic model

Email address: ibaraki@hiroshima-u.ac.jp (Soichi Ibaraki)

1. Introduction

A linear axis has translational error motions in three directions, namely the linear positioning and straightness error motions, and angular error motions around three axes, namely yaw, pitch and roll error motions [1]. In the standardized accuracy test procedures for machine tools, described in ISO 230-1 [1], each error motion is separately measured in a different setup with a different measuring instrument. For example, the linear positioning deviations is typically measured by using a laser interferometer. The straightness error motion is typically measured by a straight edge and a linear displacement sensor. The squareness error is measured by using a square. Angular error motions are measured by an autocollimator or a precision level. Typical machine tools have three or more linear axes. Full evaluation of all the error motions requires significant time and a lot of measuring instruments.

The multilateration measurement, the term in [1], enables a user to identify all the error motions by using a tracking interferometer (the term in [1]), or a laser tracker. Figure 1 illustrates its 2D version. The distance from the tracking interferometer to the retroreflector, installed on a machine spindle, is measured. By the distances from three or more tracking interferometers, based on the trilateration principle, the position of the retroreflector can be calculated (the detailed formulation will be presented in Section 2.1). By using the machine's kinematic model, all the error motions of linear axes can be estimated. This "indirect" error calibration has been long studied [2, 3, 4, 5]. Its commercial product is available (Etalon [6, 7]). Unlike more typical commercial laser trackers, where the target's 3D position is estimated by the distance to it and the orientation of the laser beam, the multilateration is based on the measured distances, and does not use the angular orientation of the laser beam in its calculation, which significantly reduces its position measurement uncertainty. All the error motions can be evaluated by using a single measuring instrument only — this is a significant practical advantage.

When four tracking interferometers are available (for the 3D case), the multilateration measurement can be done by a single setup. In practice, due

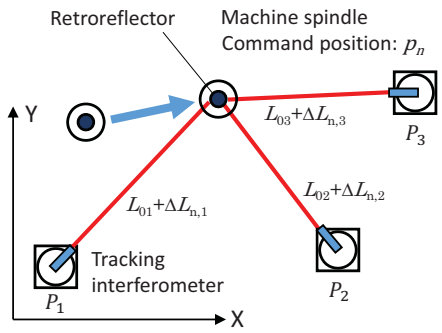

Figure 1: Typical multilateration measurement setup (2D version).

to the instrument's higher cost, many users have only one. In such a case, the same test must be repeated four times or more with different tracking interferometer positions, assuming the machine's positioning repeatability [6]. It typically takes several hours. Furthermore, more importantly, a single tracking test does not give any useful information to a user. When all the four tests are finished, all the error motions can be calculated. It is, in a sense, a "black-box" test, which outputs the results only when all the four tests are input. This can potentially limit its applications:

- The multilateration measurement can be used only for the final inspection or the numerical compensation of a completely assembled machine. During an assembly process, a machine tool builder may want to check error motions of each axis and modify the assembly accordingly. It is not possible to apply the multilateration measurement to such a quick check.

- Even if one of the tests fails or has abnormally large measurement error due to e.g. some setup error or external disturbance, it will likely not be noticed until all the tests are finished.

- Due to long measurement time, it cannot be applied to, for example, the evaluation of the thermal influence on the volumetric accuracy [8, 9].

This paper proposes a novel test scheme consisting of the following tests: 1) direct measurement of the linear positioning deviation of two linear axes, and 2) the distance measurement to the retroreflector, positioned on a rectangular path, by continuously regulating the laser beam direction of a laser interferometer. It requires a laser interferometer only. Its objective is to identify all the 2D error motions of two linear axes, i.e. the straightness deviation and the angular deviations of each linear axis, as well as the squareness error between them.

In the proposed scheme, a laser interferometer is installed on a machine spindle with a rotary axis. As the two linear axes position it on a rectangular path, the laser beam orientation is regulated by the rotary axis to the prescribed retroreflector position. The distance from the laser interferometer to the retroreflector is measured. This measurement is analogous to the laser tracker measurement. The difference is that 1) the proposed scheme requires a laser interferometer only. Lower implementation cost is its major practical advantage. 2) While the conventional multilateration requires "black-box" calculation based on all of the four tracking tests, as discussed above, the proposed scheme separately identifies a part of the error motions by each test. It can be potentially applied to a quick check or axis-to-axis accuracy check in a machine assembly or accuracy inspection.

The proposed scheme targets error motions of two linear axes on a 2D plane only. To evaluate all the 3D error motions of three linear axes (X-, Y- and Z-axes), it can be applied to all the planes, i.e. XY, YZ and ZX planes.

The conventional laser interferometer measurement is applied to a linear axis moving along a straight line. The proposed test extends it to a rectangular trajectory. In this sense, the proposed test can be seen analogous to the diagonal test [10], the step-diagonal test [11] and the multi-line tests [12, 14]. In the diagonal test, the laser beam is fixed on a diagonal of the measured volume and the machine moves on this diagonal. In the step diagonal test, the laser beam is fixed on the diagonal, and the machine moves on a step-shaped zigzag path on the diagonal. These tests are proposed to indirectly

identify error motions of linear axes by a laser interferometer only, similarly as the proposed test. The diagonal test is, however, effective only to estimate the squareness error between the two linear axes [15]. It has been clarified in [16, 17, 18, 19] that the step diagonal test fails when angular error motions are significant. In the multi-line tests, many laser beam paths, e.g. 15 [14], 21 [12] or 33-55 [13] lines, are measured. In all these tests, the laser beam is fixed. This paper's scheme enables a user to identify all the error motions of two linear axes by three tests only, by regulating the laser beam direction to follow the machine's command trajectory.

Unlike a commercial tracking interferometer, the proposed scheme does not regulate the laser beam to automatically follow the retroreflector; its orientation is regulated to the prescribed retroreflector position, i.e. in a "open-loop" control manner. The same concept, "open-loop" tracking interferometer, has been proposed by Ibaraki et al. [20, 21, 22]. In these works, it is applied to the conventional multilateration, i.e. at least four tracking tests are needed to identify all the 3D error motions of three linear axes. An original contribution of this paper is on the proposal of the test scheme requiring a single tracking test only, in addition to direct measurement of the linear positioning deviation of each axis.

2. Proposed test procedure to identify error motions of linear axes

2.1. Review: conventional multilateration algorithm

As the background, the conventional multilateration algorithm is briefly reviewed (see [6, 5] for further details). To compare with the proposed scheme, this section presents its 2D version. The X-Y plane is taken as an example.

This paper considers a machine configuration where the Y-axis is mounted on the X-axis. The objective is to estimate error motions of X- and Y-axes, shown in Table 1, for all the command positions, $x_i^* = 1, \cdots, N_x$ and $y_j^* = 1, \cdots, N_y$. See Fig. 1. Suppose that the retroreflector, attached to the machine spindle, is positioned at the n-th command position, $p_n^* = [x_{i_n}, y_{j_n}]^T$

($n = 1, \cdots, N$, $i_n \in [1, N_x]$, and $j_n \in [1, N_y]$). The tracking interferometer's rotation center is located on the machine table at $P_m^* \in \mathbb{R}^2$ ($m = 1, \cdots, N_t$). Throughout this paper, the superscript "$*$" represents the commanded value. The laser displacement from the m-th tracking interferometer to the n-th retroreflector position, $\Delta L_{n,m} \in \mathbb{R}$, is measured. The problem can be written as the following minimization problem:

$$\min_{\theta} \sum_{n=1\cdots N, m=1\cdots N_t} \left(\|\hat{p}_n - P_m\| - L_{0m} - \Delta L_{n,m} \right)^2 \tag{1}$$

where:

$$\begin{aligned} \hat{p}_n &= p_n^* + \\ &\left[\begin{array}{l} E_{XX}(x_{i_n}^*) + E_{XY}(y_{j_m}^*) - \left(E_{CX}(x_{i_n}^*) + E_{C(0X)Y} \right) y_{j_m}^* \\ E_{YX}(x_{i_n}^*) + E_{YY}(y_{j_m}^*) \end{array} \right] \end{aligned} \tag{2}$$

and $L_{0m} \in \mathbb{R}$ represents the dead path length in the measurement by the m-th tracking interferometer [6]. Eq. (2) represents this machine configuration's kinematic model. It is the basis for many previous publications on indirect measurement for machine tools [23]. $\theta \in \mathbb{R}^{3N_x+2N_y+1+3N_t}$ represents a set of unknown parameters to be identified:

$$\begin{aligned} \theta = \Big[& \left\{ E_{XX}(x_i^*), E_{YX}(x_i^*), E_{CX}(x_i^*) \right\}_{i=1,\cdots,N_x}, \\ & \left\{ E_{YY}(y_j^*), E_{XY}(y_j^*) \right\}_{j=1,\cdots,N_y}, E_{C(0X)Y}, . \\ & \left\{ P_m \right\}_{m=1,\cdots,N_t}, \left\{ L_{0m} \right\}_{m=1,\cdots,N_t} \Big] \end{aligned} \tag{3}$$

In addition to the error motions in Table 1, actual tracking interferometer positions, $P_m \in \mathbb{R}^2$, and the dead path lengths, L_{0m}, are identified. Typically, the problem (1) is locally solved by an iterative nonlinear least square method. It can be solved when the tracking interferometer is placed at three or more different locations. i.e. $N_m \geq 3$, in the 2D case.

Table 1: 2D error motions of X- and Y-axes [1].

$E_{XX}(x_i^*)$	Linear positioning deviation of X-axis at $x = x_i^*$
$E_{YX}(x_i^*)$	Straightness deviation of X-axis at $x = x_i^*$
$E_{CX}(x_i^*)$	Angular error motion of X-axis around Z-axis at $x = x_i^*$
$E_{YY}(y_j^*)$	Linear positioning deviation of Y-axis at $y = y_j^*$
$E_{XY}(y_j^*)$	Straightness deviation of Y-axis at $y = y_j^*$
$E_{C(0X)Y}$	Squareness error of Y- to X-axis

2.2. Proposed test procedure

The proposed scheme does not use a tracking interferometer. This paper considers a five-axis machine tool of the configuration shown in Fig. 2. A laser interferometer is attached on the spindle's face plate such that the laser beam approximately intersects with the C-axis of rotation (see Fig. 2). The intersection of the C-axis and the laser beam is called *the spindle's reference point* hereafter. By rotating the C-axis, the laser beam can be directed on the vertical XY plane. A retroreflector is placed to the work table. A cat's eye retroreflector is typically used, which is a spherical glass of sufficiently high geometric accuracy with its hemispheric surface coated by the total-reflection metal-film deposition [24].

This paper proposes the following procedure:

1) The linear positioning deviation of the X-axis is measured at $p_{1,i}^* = [x_i^*, y_a^*]$ $(i = 1, \cdots, N_x,\ a \in [1, N_y])$. This can be done by fixing the laser beam in the X-direction toward the retroreflector. The retroreflector is placed on the measured line, $y = y_a^*$, and its position is denoted by $P_1^* \in \mathbb{R}^2$. See Fig. 2a.
2) Similarly, the linear positioning deviation of the Y-axis is measured at $p_{2,j}^* = \left[x_b^*, y_j^*\right]$ $(j = 1, \cdots, N_y)$. The retroreflector is at $P_2^* \in \mathbb{R}^2$. See Fig. 2b.
3) The tracking test: the spindle's reference point is positioned at the given set of command positions, $p_{3,n}^* = (x_{i_n}^*, y_{j_n}^*)$ $(n = 1, \cdots, N,\ i_n \in [1, N_x]$, and $j_n \in [1, N_y])$. The C-axis is regulated such that the laser

beam is directed to the pre-estimated retroreflector position, $P_3^* \in \mathbb{R}^2$. The laser displacement to it, $\Delta L_{3,n} \in \mathbb{R}$, is measured. See Figs. 2c and d.

In Step 3), the C-axis angular position can be calculated under the following assumption: 1) the retroreflector's position, $P_3^* \in \mathbb{R}^2$, is roughly estimated. 2) When $C = 0°$, the laser beam is approximately parallel to the machine's Y-axis. Then, by indexing the C-axis at:

$$c_{3,n}^* = \tan^{-1}\left(-\frac{P_3^*(1) - p_{3,n}^*(1)}{P_3^*(2) - p_{3,n}^*(2)}\right) \tag{4}$$

then the laser beam is nominally directed to the retroreflector (see Fig. 3).

Clearly, when there exists an error in the spindle position, $p_{3,n}^*$, or the retroreflector position, P_3^*, then the laser beam would not be directed exactly to the retroreflector center. The C-axis angular positioning error also contributes to this laser beam direction error. It imposes, however, only the "cosine error" on the laser displacement. In the application to machine tool calibration, it is reasonable to assume that the machine's positioning error is sufficiently small to make its "cosine error" negligibly small. The influence on the laser beam orientation error on the uncertainty in the proposed scheme will be studied in Section 4.

Remark #1: The elimination of an automated tracking mechanism by regulating the laser beam to nominal target positions was proposed by Ibaraki et al. in [20, 21, 22] and it is not this paper's original contribution. Refs. [20, 21, 22] apply it to the conventional multilateration algorithm reviewed in Section 2.1. The proposal of the three-step test procedure in Fig. 2, as well as the new multilateration formulation in Section 2.3, is an original contribution of this paper.

Remark #2: In the proposed test setup in Fig. 2, a laser interferometer is installed in the spindle side and a retroreflector is fixed on the work table at three different positions. When an automated tracking interferometer is available, exactly the same test can be performed with the tracking in-

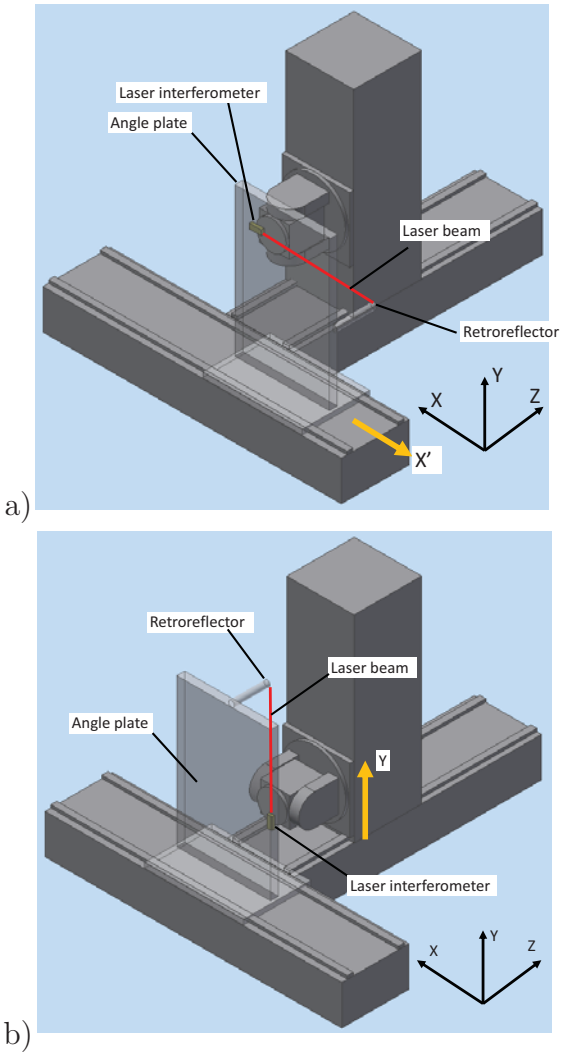

Figure 2: Proposed test procedure. a) Direct measurement of X-axis linear positioning deviation, and b) Y-axis linear positioning deviation.

c)

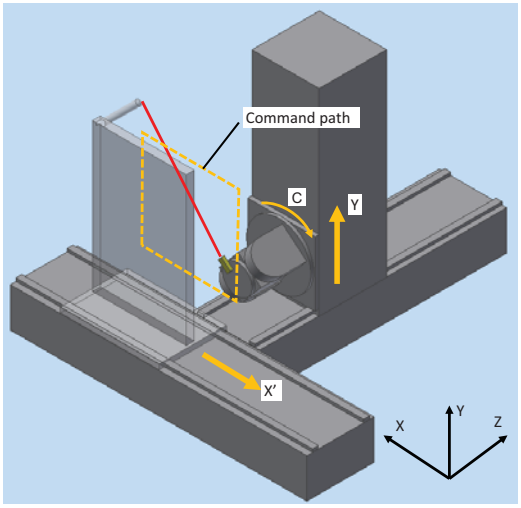

d)

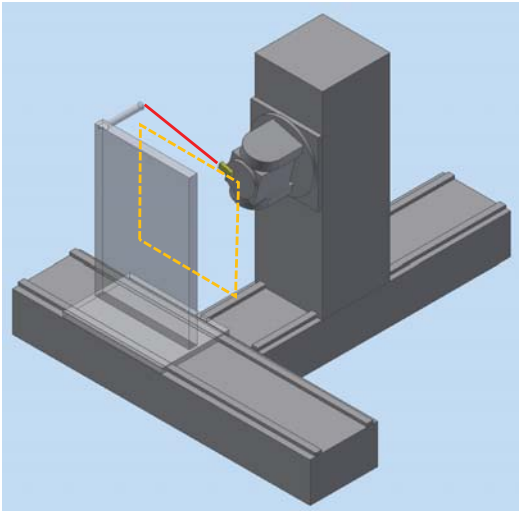

Figure 2 (Continued): Proposed test procedure. c) and d) the "open-loop" tracking test for the square path.

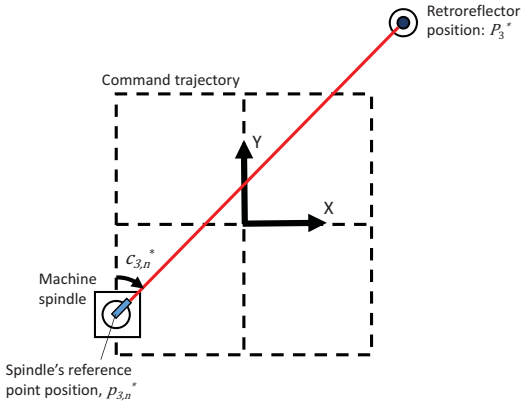

Figure 3: Setup for the proposed tracking test.

terferometer installed on the work table at three different position, and a retroreflector is in the spindle side. This setup is very similar to the one depicted in Fig. 1. The proposed three-step test procedure, as well as the algorithm proposed in Section 2.3, can be applied to this setup with an automated tracking interferometer. This setup is presented in [9].

Remark #3: To calculate Eq. (4), the retroreflector position, P_3^*, must be estimated in priori. See [22] for an example estimation procedure.

Remark #4: Major setup errors include the intersection error of the laser beam to the C-axis of rotation. In the experiment, as will be described in Section 3.1, the laser interferometer is mounted on a screw-driven stage such that its position can be adjusted. The intersection error can be minimized by the following procedure: the laser beam is aligned to the retroreflector center such that the distance to it can be measured. Then, rotate the C-axis within the small range where the distance is measurable. Adjust the laser interferometer position such that the variation in the measured distance is minimized.

Other setup errors include: 1) the squareness error of the laser beam to the C-axis and 2) the estimation error of the retroreflector position (see Remark #2). Their influence is minor ("cosine error"). It will be quantitatively

analyzed in Section 4.

2.3. Algorithm to estimate linear axis error motions

In Step 1), the kinematic model in Eq. (2), representing the relationship between the modelled position, $p^*_{1,i} \in \mathbb{R}^2$, and the command position, $p^*_{1,i} = [x^*_i, y^*_a]$, under θ in Eq. (3), can be rewritten by

$$\hat{p}_{1,i} = p^*_{1,i} + A_{\text{kinematic},1,i} \cdot \theta \tag{5}$$

where $A_{\text{kinematic},1,i} \in \mathbb{R}^{2\times(3N_x+2N_y+1+3N_t)}$ is constructed from Eqs. (2) and (3). The laser displacement measured at $p^*_{1,i} = [x^*_i, y^*_a]$ is denoted by $\Delta L_{1,i} \in \mathbb{R}$. Step 2) is formulated similarly.

In the step 3), for the given command position, $p^*_{3,n} = (x^*_{i_n}, y^*_{j_n})$, rewrite the kinematic model in Eq. (2) by using θ in Eq. (3) as follows:

$$\hat{p}_{3,n} = p^*_{3,n} + A_{\text{kinematic},3,n} \cdot \theta \tag{6}$$

The laser displacement measured at $p^*_{3,n}$ is denoted by $\Delta L_{3,n} \in \mathbb{R}$. Then, θ in Eq. (3) can be identified by solving the following problem:

$$\begin{aligned}\min_{the[ta} \Bigg\{ &\sum_{i=1}^{N_x} \left(\|\hat{p}_{1,i} - P_1\| - L_{01} - \Delta L_{1,i}\right)^2 + \\ &\sum_{j=1}^{N_y} \left(\|\hat{p}_{2,j} - P_2\| - L_{02} - \Delta L_{2,j}\right)^2 + \\ &\sum_{n=1}^{N} \left(\|\hat{p}_{3,n} - P_3\| - L_{03} - \Delta L_{3,b}\right)^2 \Bigg\}\end{aligned} \tag{7}$$

Analogously to Section 2.1, this can be locally solved by an iterative approach.

Remark: $E_{XX}(x^*_i) = \Delta L_{1,i}$ (or $E_{YY}(y^*_j) = \Delta L_{2,j}$) only when $y^*_a = 0$ ($x^*_b = 0$). Eqs. (6) and (5) formulate a general case for any y^*_a (x^*_b).

Remark #2: In the problem (7), the retroreflector positions in Steps 1)

and 2) should be constrained by : $P_1(2) = y_a^*$ and $P_2(1) = x_a^*$. Furthermore, the following constraints are needed to uniquely define the coordinate system and error motions [5]:

$$\begin{aligned} E_{XX}(x_{i0}) &= E_{YX}(x_{i0}) = E_{CX}(x_{i0}) = E_{XY}(y_{i0}) = E_{YY}(y_{i0}) = 0 \\ E_{YX}(x_{N_x})) &= E_{XY}(y_{N_y}) = 0 \end{aligned} \tag{8}$$

where (x_{i0}, y_{i0}) represents the origin, where all the error motions are defined zero.

3. Experiment

3.1. Experimental setup

Figure 4a shows the experimental setup (Step 3 in Section 2.2). Figure 4b shows the laser interferometer attached to the spindle face plate. Its position in the plane vertical to the C-axis can be adjusted such that the laser beam approximately intersects with the C-axis (see Remark #3 in Section 2.2). Major specifications of the laser interferometer and the cat's eye retroreflector are shown respectively in Tables 2 and 3.

3.2. Identified linear axis error motions

Figure 5 shows the command trajectory of spindle's reference point, as well as the retroreflector positions. First, the linear positioning deviation of X-axis, $\Delta L_{1,i}$, was measured at $x_i = -400, -300, \cdots, 400$ mm ($N_x = 9$), with the retroreflector at P_1^* in Fig. 5 (Step 1 in Section 2.2 and Fig. 2a). Then, the linear positioning deviation of Y-axis, $\Delta L_{2,j}$, was measured at $y_j = -400, -300, \cdots, 400$ mm ($N_y = 9$) with the retroreflector at P_2^* in Fig. 5 (Step 2 in Section 2.2 and Fig. 2b). Figure 6 shows the measured linear positioning deviations for a) X- and b) Y-axes.

Then, the proposed "open-loop" tracking test (Step 3 in Section 2.2 and Figs. 2c and d) was performed with the retroreflector at P_3 in Fig. 5. Figure 7a shows the measured laser displacement profile, $\Delta L_{3,n}$ ($n = 1, \cdots, N =$

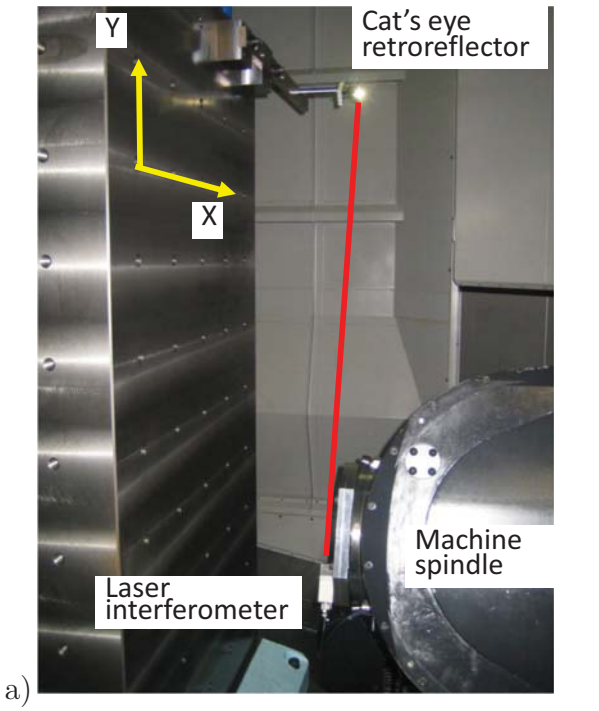

a)

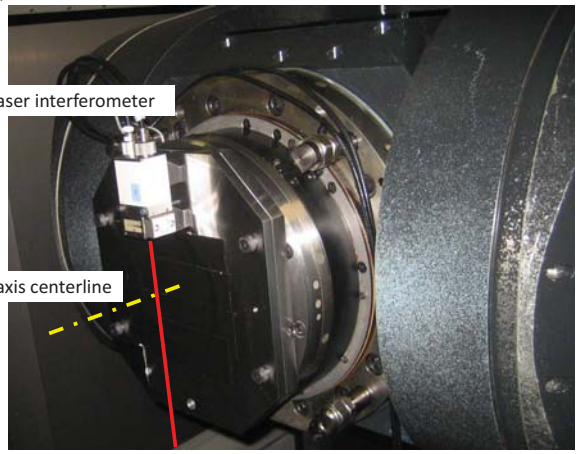

b)

Figure 4: Experimental setup. a) Setup in the tracking test, b) a laser interferometer attached to the machine's spindle face plate.

53), for the command trajectory, $p^*_{3,n}$, shown in Fig. 5. Figure 7b shows the difference of the measured laser displacement profile, $\Delta L_{3,n}$, to its nominal

Table 2: Major specifications of the laser interferometer (Distax L-IH-302A by Tokyo Seimitsu Co., Ltd.).

Laser	He-Ne laser (vacuum wavelength 633.0 nm)
Measurement range	10 m
Measurement resolution	$\lambda/64$ ($\approx 0.01\mu$m)
Maximum response speed	630 $\sec^{-1}$
Measurement uncertainty	$\pm(\lvert L\rvert \times 10^{-7} + 0.005 \times 10^{-6})$ m where L is the measurement length.

Table 3: Major specifications of the cat's eye retroreflector (by Etalon AG).

Viewing angle	$\pm 80^\circ$
Optical form deviation (circularity	$< 0.2\mu$m

length, $\|p^*_{3,n} - P^*_3\|$, when assumed no error motion of X- and Y-axes. The proposed algorithm in Section 2.2 identifies θ in Eq. (3) such that this difference is minimized.

Figure 8 shows linear axis error motions estimated by applying the proposed algorithm, a) the straightness deviation of X-axis in Y-direction, $E_{YX}(x^*_i)$, b) the pitch error motion of X-axis around Z-axis, $E_{CX}(x^*_i)$, and c) the straightness deviation of Y-axis in X-direction, $E_{XY}(y^*_j)$. Figure 9 shows spindle reference positions estimated by the kinematic model in Eq. (2) with identified error motions shown in Fig. 8.

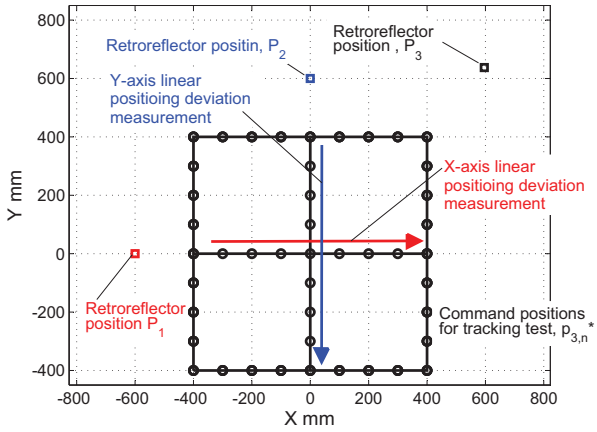

Figure 5: Command positions of spindle's reference point and the cat's eye retroreflector positions.

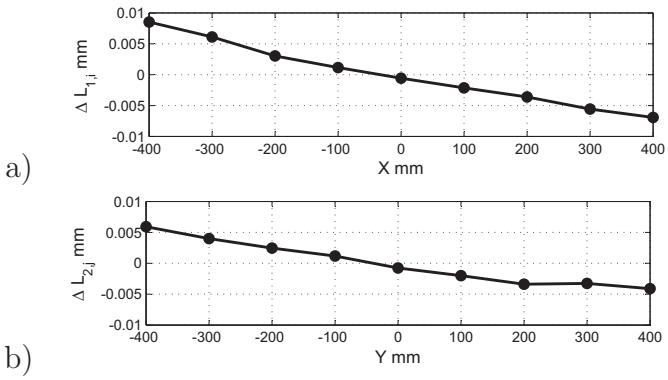

Figure 6: Measured linear positioning deviation of a) X-axis, $\Delta L_{1,i}$, and b) Y-axis, $\Delta L_{2,j}$. The horizontal axis represents the command X- (Y-) axis positions, x_i^* (y_j^*)

.

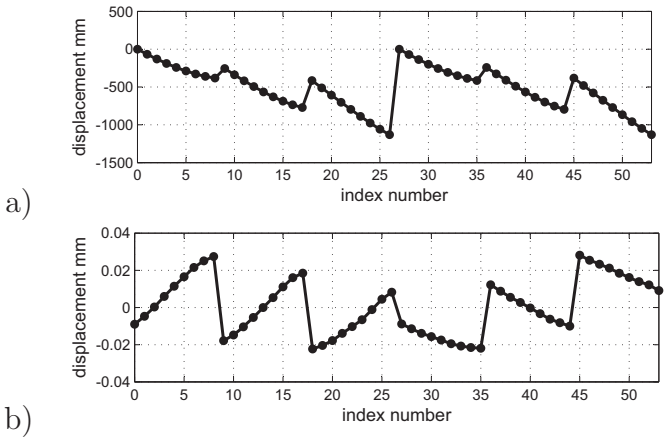

Figure 7: a) Measured laser displacement profile by the proposed "open-loop" tracking interferometer measurement, $\Delta L_{3,n}$ $(n = 1, \cdots, N)$. b) The difference of the measured laser displacement profile a) to its nominal length, $\|p^*_{3,n} - P^*_3\|$, assuming no geometric error of the machine tool.

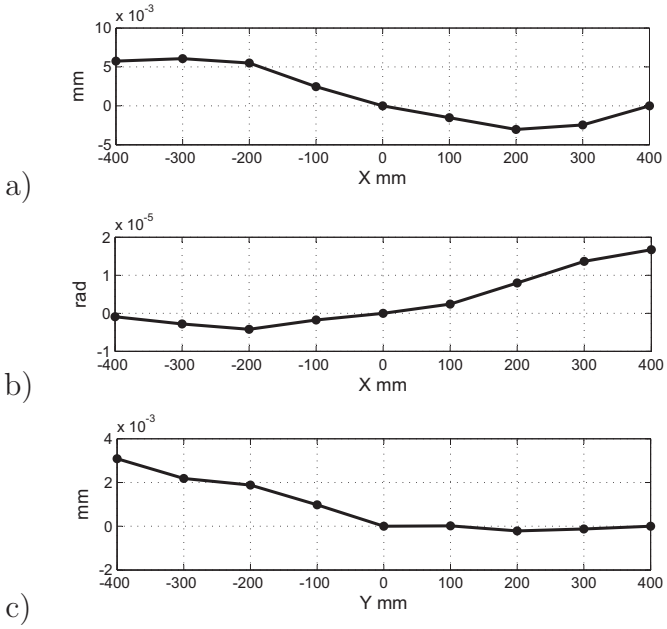

Figure 8: Estimated linear axis error motions by the proposed algorithm. a) The straightness deviation of X-axis in Y-direction, $E_{YX}(x_i^*)$, b) the pitch error motion of X-axis around Z-axis, $E_{CX}(x_i^*)$, and c) the straightness deviation of Y-axis in X-direction, $E_{XY}(y_j^*)$.

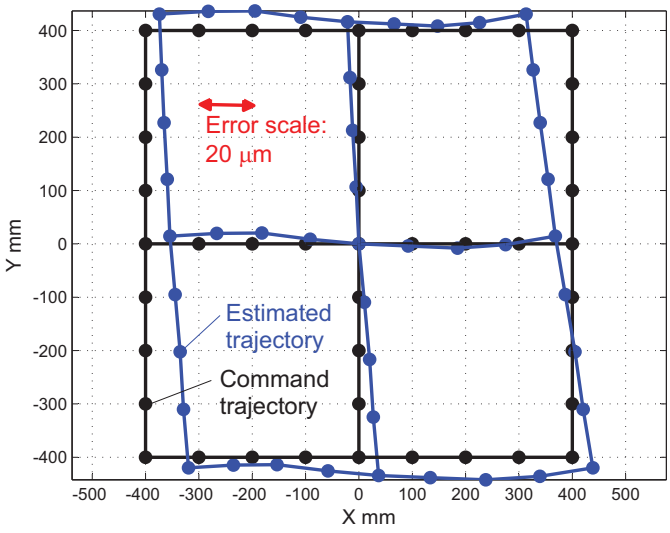

Figure 9: Estimated spindle reference point positions by the proposed scheme. The error between estimated and command positions is magnified 5,000 times (see "Error scale").

Table 4: Comparison of the squareness error of Y- to X-axis, $E_{C(0X)Y}$, directly measured by using a square, with the one estimated by the proposed scheme.

	Measured	Estimated
$E_{C(0X)Y}$	-12.0 μm/m	-7.2 μm/m

3.3. Experimental validation

The validity of a part of the estimated error motions was experimentally investigated by comparing with other direct measurements. First, the squareness error of Y- to X-axis, $E_{C(0X)Y}$, was measured according to ISO 230-1 [1] by using a square and a dial gauge (see Fig. 10 for the measurement setup). A square of the size 550×500 mm was used. The squareness was measured approximately at $(X, Y) = (0, 0)$ (measured lines: $(X, Y) = (-547 \sim -22, -31)$ mm and $(X, Y) = (3, -576 \sim -40)$ mm). Table 4 compares the measured squareness error to the estimate by the proposed scheme. They show a good match. According to the square's calibration chart by its manufacturer, the uncertainty in the calibrated perpendicularity of the square is 2.0 $\mu m/550$ mm. The difference in measured and estimated squareness errors Table 4 is close to this uncertainty. Note that the measured ranges are different (the proposed scheme: 800×800 mm, the square: 525×536 mm) due to the unavailability of a larger square. The measured lines to define the squareness error are also slightly different.

Furthermore, the pitch error motion of X-axis, $E_{CX}(x_i^*)$, was directly measured by using a precision level (DL-S3 by Niigata Seiki Co., Ltd.), Figure 11 shows its comparison with the estimates by the proposed scheme. The measured $E_{CX}(x_i)$ is defined zero at $x_i^* = 0$. A level measures the physical orientation of the machine table, while the proposed scheme estimates $E_{CX}(x_i^*)$ from the orientation of Y-axis motion at x_i^*. Slight difference observed in Fig. 11 may be attributable to it.

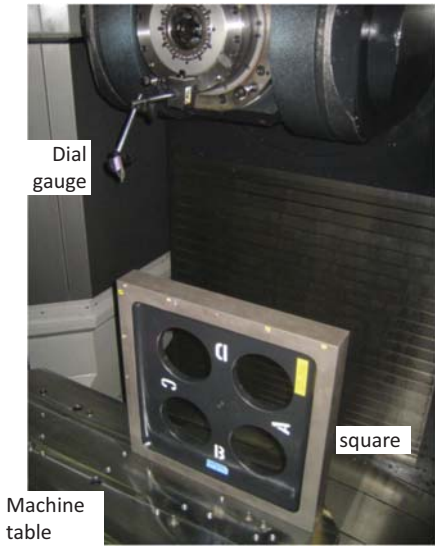

Figure 10: Measurement setup of the squareness error.

4. Uncertainty analysis

4.1. Objective of uncertainty analysis

The proposed test procedure has uncertainty contributors that are in principle negligible in conventional automated tracking interferometers. For example, since the laser beam direction is regulated by Eq. (4), when there exists the machine tool's positioning error, i.e. an error with $p^*_{3,n}$ in Eq. (4), the laser beam would not be directed exactly to the center of the retroreflector. The angular positioning error of C-axis, as well as an error in the initial estimate of the retroreflector position, P^*_3 in Eq. (4), also contributes to the laser beam orientation error. In conventional tracking interferometers with an automated tracking mechanism, this contribution can be negligibly small, when the tracking accuracy is sufficiently high.

To validate the proposed scheme, it is important to show that the uncertainty contributors, existing only in the "open-loop" tracking measurement, do not impose significant influence on the overall measurement uncertainty, when the machine tool, as well as the measuring instrument and its setup,

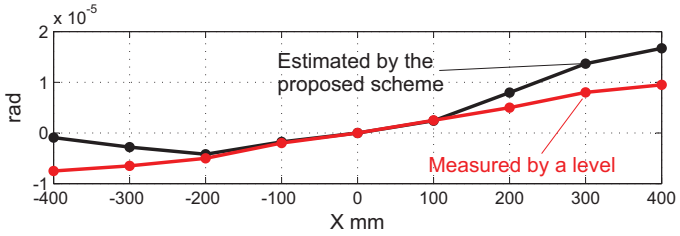

Figure 11: Comparison of the pitch error motion of X-axis, $E_{CX}(x_i)$, directly measured by using a level, with the one estimated by the proposed scheme.

has "typical" accuracy. The uncertainty analysis presented in this section is analogous to the ones presented in the authors' previous works [22, 20, 21].

4.2. Uncertainty budget for laser displacements

Table 5 shows the uncertainty, $U(k = 1)$, of the laser displacement when the retroreflector is at P_3^*, and the spindle reference point is at (X, Y)=(-400, -400) mm in Fig. 5. The uncertainty in the laser displacement significantly depends on the machine position, and Table 5 merely shows an example for a single point to illustrate each contributor's influence. "Type A" uncertainties are assessed by actually measuring the experimental instrument. "Type B" uncertainties are assessed by using the instrument's catalog or specifications.

In Table 5, u_{41}, u_{43} and u_{44} are in principle negligible in the conventional automated tracking interferometers, but inherently exist in the proposed scheme (see [22, 20, 21]). Although this uncertainty in the laser beam direction can be significant, its contribution to the laser displacement is sufficiently small (u_4), since it gives only the "cosine error."

The contributors, u_1, u_2, and u_{42} can be in principle present also in automated tracking interferometers. The present analysis validates that the "open-loop" regulation of laser beam direction does not significantly contribute on the uncertainty of the multilateration measurement.

4.3. Uncertainty in spindle position estimation

The uncertainty in the laser displacement at each command position propagates into the uncertainty in the estimated spindle positions. This relationship cannot be analytically formulated, since it involves the numerical optimization in Eq. (7). In such a case, the Monte Carlo simulation can be applied for the uncertainty evaluation [25]. Analogous analysis is presented in [26, 21, 22].

Figure 12 shows the uncertainty ($k = 2$) in the estimated spindle positions, $\hat{p}_n$, calculated by Eq. (2). The Monte Carlo simulation was performed 10,000 times.

The uncertainty is zero at $(x, y) = (0, 0)$ due to the constraint in Eq. (8). The uncertainty is smaller at $y = 0$ since the X-axis pitch error motion, $E_{CX}(x_i^*)$, does not influence there. The sensitivity of the measured laser displacement in the tracking test (Step 3) on the straightness deviations of X- and Y-axes, $E_{YX}(x_i^*)$ and $E_{XY}(y_j^*)$, and the angular deviation of X-axis, $E_{CX}(x_i^*)$, depends on the angle between the error direction and the laser beam direction at each command point. For example, when the laser beam direction in the tracking test (Step 3) is closer to either X- or Y-direction, this sensitivity on the straightness deviation in the Y-direction, $E_{YX}(x_i^*)$, decreases. This causes higher uncertainty at $(x, y) = (-400, 400)$ and $(400, -400)$ in Fig. 12. Clearly, the uncertainty significantly depends on the retroreflector position in the tracking test (P_3 in Fig. 5).

5. Conclusion

The conventional multilateration enables a user to evaluate all the error motions of three linear axes by using a single measuring instrument only, which is its strong advantage. On the other hand, unlike conventional standardized measurement procedures, where individual error motion is independently measured in a different setup, all the error motions can be calculated only when all the four tests are finished. It is, in a sense, a "black-box" test, where a single tracking test does not give any useful information to a

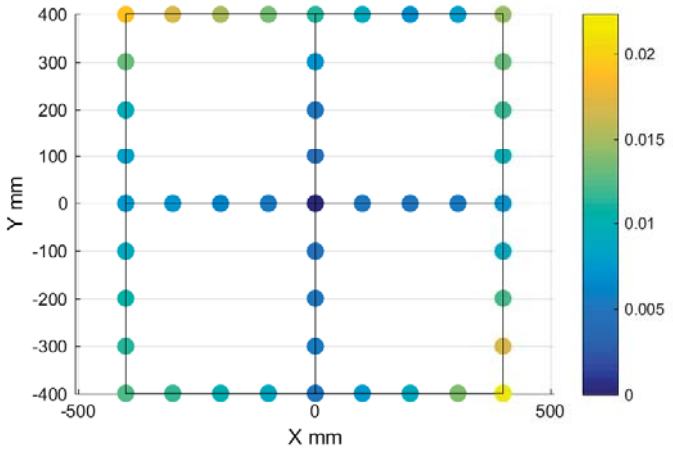

Figure 12: Assessed uncertainty in estimated target positions propagated from the uncertainty in laser displacements shown in Table 5. The color represents the uncertainty ($k = 2$) of the distance of the estimated target position to its command position.

user. To perform the multilateration, an expensive tracking interferometer is needed. They are disadvantages with the multilateration test.

This paper proposes a novel scheme to identify straightness deviations and angular deviations of two linear axes by a single tracking test, when the linear positioning deviation of each axis is separately measured. Since the proposed scheme uses the machine's rotary axis to regulate the laser beam direction, it requires a laser interferometer only, with no specialized tracking mechanism for an automated tracking interferometer. Its disadvantage is that it is limited to a 2D plane. To identify all the 3D error motions of three linear axes, three tests to measure the linear positioning deviation of X-, Y- and Z-axes, and three tracking tests for rectangular paths on XY, YZ, and ZX planes are needed.

In the experiment, a part of the error motions estimated by the proposed scheme was experimentally validated by comparing with a conventional direct measurement. Generally, such a comparative measurement can only validate the estimates within each measurement's uncertainty and the machine's repeatability. This paper presents the uncertainty analysis to evaluate

Table 5: Error budget for laser displacement uncertainty ($k = 1$) at the spindle position $(X, Y) = (-400, -400)$ mm and the interferometer position P_3^* (see Fig. 5).

Symbol		Contributor	Contribution to laser displacement uncertainty	Type
u_1	Uncertainty in laser length		0.65 μm	
	u_{11}	Wavelength accuracy	0.03 μm	B
	u_{12}	Wavelength correction	0.16 μm	B
	u_{13}	Environmental change	0.08 μm	A
	u_{14}	Machine's Repeatability	0.63 μm	A
u_2	Uncertainty in interferometer position in laser direction		2.12 μm	
	u_{21}	Radial error motion of C-axis	2.12 μm	A
u_3	Uncertainty in interferometer position error in direction normal to laser		≈ 0 μm	
u_4	Uncertainty due to laser beam orientation error		0.14μm	
	u_{41}	Uncertainty in C-axis zero angular position	2.88×10^{-4} rad	B
	u_{42}	Angular positioning error of C-axis	0.18×10^{-4} rad	A
	u_{43}	Error in estimated retroreflector position	6.73×10^{-4} rad	A
	u_{44}	Uncertainty due to machine tool positioning error	0.34×10^{-4} rad	A

the propagation of uncertainty contributors, with a particular focus on the contributors inherently present in the proposed "open-loop" tracking interferometer test.

References

[1] ISO 230-1:2012, Test code for machine tools – Part 1: Geometric accuracy of machines operating under no-load or quasi-static conditions.

[2] G.N. Peggs, Virtual technologies for advanced manufacturing and metrology, Int'l J. of Computer Integrated Manufacturing, 16(7/8) (2003).

[3] E.B. Hughes, A. Wilson, G.N. Peggs, Design of a high-accuracy CMM based on multi-lateration techniques, Ann. CIRP – Manuf. Technol. 49(1) (2000) 391-394.

[4] S. Aguado, D. Samper, J. Santolaria, J. J. Aguilar, Identification strategy of error parameter in volumetric error compensation of machine tool based on laser tracker measurements, Int'l J of Machine Tools and Manufacture, 53(1) (2012) 160-169.

[5] S. Ibaraki, T. Kudo, T. Yano, T. Takatsuji, S. Osawa, O. Sato, Estimation of three-dimensional volumetric errors of machining centers by a tracking interferometer, Precis. Eng. 39 (2014) 179-186.

[6] H. Schwenke, M. Franke, J. Hannaford, H. Kunzmann, Error mapping of CMMs and machine tools by a single tracking interferometer, Ann. CIRP – Manuf. Technol., 54(1) (2005) 475-478.

[7] H. Schwenke, R. Schmitt, P. Jatzkowski, C. Warmann, On-the-fly calibration of linear and rotary axes of machine tools and CMMs using a tracking interferometer, Ann. CIRP – Manuf. Technol., 58(1) (2009) 477-480.

[8] E. Gomez-Acedo, A. Olarra, M. Zubieta, G. Kortaberria, E. Ariznabarreta, L. N. López de Lacalle, Method for measuring thermal distortion in large machine tools by means of laser multilateration, Int'l J of Advanced Manufacturing Technology, 80 (2015) 523-534

[9] S. Ibaraki, P. Blaser, M. Shimoike, N. Takayama, M. Nakaminami, Y. Ido, Measurement of thermal influence on a two-dimensional motion trajectory using a tracking interferometer, Ann. CIRP – Manuf. Technol., 65(1) (2016) 483-486.

[10] ISO 230-6:2002, Test code for machine tools – Part 6: Determination of positioning accuracy on body and face diagonals (Diagonal displacement tests)

[11] C. Wang, Laser vector measurement technique for the determination and compensation of volumetric positioning errors. Part 1: Basic theory, Review of Scientific Instruments, 71(10) (2000) 3933-3937.

[12] G. Chen, J. Yuan, and J. Ni, A displacement measurement approach for machine geometric error assessment. Int'l J of Machine Tools and Manufacture, 41(1) (2001) 149-161.

[13] P. Pedone, E. Audrito, A. Balsamo, Compensation of CMM geometrical errors by the GEMIL techniqueExperimental results, Ann. CIRP – Manuf. Technol., 63(1) (2014) 489-492.

[14] S. Zhu, G. Ding, S. Qin, J. Lei, L. Zhuang, K. Yan, Integrated geometric error modeling, identification and compensation of CNC machine tools, Int'l J of Machine Tools and Manufacture, 52(1) (2012) 24-29.

[15] M. A. V. Chapman, Limitations of laser diagonal measurements, Precis. Eng., 27(4) (2003) 401-406.

[16] S. Ibaraki, T. Hata, and Matsubara, A new formulation of laser step-diagonal measurement – two-dimensional case, Precis. Eng., 33(1) (2009) 56-64.

[17] S. Ibaraki and T. Hata, A new formulation of laser step diagonal measurement – Three-dimensional case, Precis. Eng., 34(3) (2010) 516-525.

[18] C. B. Bui, J. Hwang, C-H Lee, C-H Park, Three-face step-diagonal measurement method for the estimation of volumetric positioning errors in a 3D workspace, Int'l J of Machine Tools and Manufacture, 60 (2012) 40-43.

[19] H. Li, P. Zhang, M. Deng, S. Xiang, Z. Du, J. Yang, Volumetric error measurement and compensation of three-axis machine tools based on laser bidirectional sequential step diagonal measuring method, Measurement Science and Technology, 31(5) (2020).

[20] S. Ibaraki, G. Sato, K. Takeuchi, ‘ Open-loop ’ tracking interferometer for machine tool volumetric error measurement – Two-dimensional case, Precis. Eng. 38(3) (2014) 666-672.

[21] S. Ibaraki, K. Nagae, G. Sato, Proposal of‘‘ open-loop ’’tracking interferometer for machine tool volumetric error measurement, Ann. CIRP – Manuf. Technol. 63(1) (2014) 501-504.

[22] S. Ibaraki, K. Tsuboi, ’Open-loop ’ tracking interferometer measurement using rotary axes of a five-axis machine tool, IEEE/ASME Trans. Mechatronics, 22(5) (2017) 2342-2350.

[23] S. Ibaraki, W. Knapp, Indirect measurement of volumetric accuracy for three-axis and five-axis machine tools: a review. Int. J. Autom. Technol. 6(2) (2012) 110-124.

[24] T. Takatsuji, M. Goto, S. Osawa, R. Yin, T. Kurosawa, Whole-viewing-angle cat's-eye retroreflector as a target of laser trackers, Measurement Science and Technology, 10(7) (1999) 87-90.

[25] JCGM 101:2008, Evaluation of measurement data – Supplement 1 to the “Guide to the expression of uncertainty in measurement” – Propagation of distributions using a Monte Carlo method

[26] B. Bringmann, J. Besuchet, and L. Rohr L, “Systematic Evaluation of Calibration Methods.” *CIRP Annals – Manufacturing Technology*, vol. 57, no.1, pp. 529-532, 2008.